

Constraining Type Ia supernovae via their distances from spiral arms

Arpine G. Karapetyan*

Center for Cosmology and Astrophysics, Alikhanian National Science Laboratory, 2 Alikhanian Brothers Str., 0036 Yerevan, Armenia

Accepted 2022 October 5. Received 2022 September 29; in original form 2022 September 6

ABSTRACT

We present an analysis of the distribution of 77 supernovae (SNe) Ia relative to spiral arms of their Sab–Scd host galaxies, using our original measurements of the SN distances from the nearby arms, and study their light curve decline rates (Δm_{15}). For the galaxies with prominent spiral arms, we show that the Δm_{15} values of SNe Ia, which are located on the arms, are typically smaller (slower declining) than those of interarm SNe Ia (faster declining). We demonstrate that the SN Ia distances from the spiral arms and their galactocentric radii are correlated: before and after the average corotation radius, SNe Ia are located near the inner and outer edges (shock fronts) of spiral arms, respectively. For the first time, we find a significant correlation between the Δm_{15} values and SN distances from the shock fronts of the arms (progenitor birthplace), which is explained in the frameworks of sub-Chandrasekhar-mass white dwarf explosion models and density wave theory, where, respectively, the Δm_{15} parameter and SN distance from the shock front are appropriate progenitor population age (lifetime) indicators.

Key words: supernovae: individual: Type Ia – galaxies: spiral – galaxies: star formation – galaxies: stellar content.

1 INTRODUCTION

Type Ia supernovae (SNe Ia) are thought to be preceded by carbon-oxygen white dwarfs (WDs) in close binaries, while the characteristics of the progenitors and the explosion channels are still up for debate (e.g. Livio & Mazzali 2018). It is now evident that SNe Ia are not a homogeneous population of WD explosions, instead they exhibit photometric and spectroscopic diversities (e.g. Taubenberger 2017). One of the characteristic parameters of SNe Ia is the difference in B -band magnitudes between the max and 15 day, or the so-called SN light curve (LC) decline rate Δm_{15} , which is practically extinction-independent (e.g. Phillips et al. 1999). There is a correlation between this parameter and SN Ia luminosities at the maximum light: SNe Ia with larger Δm_{15} values, or faster declining LCs, are fainter (Phillips 1993). The two most prevalent subclasses of peculiar SNe Ia are 91bg-like events, which are ~ 2 mag subluminous at the B -band maximum than normal SNe Ia and have fast-declining LCs, and 91T-like SNe, which are ~ 0.6 mag overluminous than normal ones and have slow-declining LCs (see Taubenberger 2017).

Theoretically, in sub-Chandrasekhar-mass (sub- $M_{\text{Ch}} < 1.4M_{\odot}$) explosion models, the luminosity of SN Ia is closely proportional to the exploding WD’s mass (e.g. Sim et al. 2010; Blondin et al. 2017): WD in a double-degenerate system, which has mass lower than M_{Ch} may, under appropriate circumstances, explodes as fainter SN Ia with faster declining LCs (Shen et al. 2017, 2021). Note that, in comparison to WD around the M_{Ch} mass, WD with a lower mass comes from a main-sequence progenitor star with a lower mass and consequently with a longer lifetime (older progenitors).

From host galaxy studies, significant correlations are observed between SN Ia LC decline rate and the global ages of their hosts or lo-

cal age at SN explosion sites (e.g. Gupta et al. 2011; Pan et al. 2014; Campbell et al. 2016; Rigault et al. 2020; Hakobyan et al. 2020, hereafter H20). On average, SNe Ia with larger Δm_{15} values are associated with older stellar environments. On the other hand, important relationships between host stellar population and properties of SNe Ia progenitors can be found by looking at the distribution of SNe Ia relative to spiral arms of galaxies (e.g. Petrosian et al. 2005; Aramyan et al. 2016, hereafter A16). It is worth noting that, according to the spiral density wave (DW) theory (Lin & Shu 1964; Roberts 1969), star formation (SF) typically occurs at shock fronts near the edges of spiral arms. From these regions, newly born SN progenitors move in the same direction as the disc rotation with respect to the spiral pattern until they reach their explosion sites (e.g. Mikhailova et al. 2007; A16). The distance from the spiral arm/from progenitor birthplace is a potential indicator of SN Ia progenitor lifetime and thus can be used to constrain SN Ia progenitors. However, SN Ia LC decline rates have never been examined in SN studies based on where they are located on spiral arms or between, as well as Δm_{15} as a function of the mentioned distance. In this *Letter*, we link the Δm_{15} and SN Ia distributions relative to spiral arms of nearby host galaxies and demonstrate, for the first time, how this could provide another interesting way to study the properties of SN Ia progenitors.

2 SAMPLE SELECTION AND REDUCTION

The database of this study consists of SNe Ia from the sample of H20, after applying the restrictions described below. Note that H20 database is a compilation of 407 nearby SNe Ia ($z \lesssim 0.036$) with known spectroscopic subclasses and B -band LC decline rates (Δm_{15}). In addition, the database contains information on the distances of SNe Ia host galaxies, morphologies, $ugriz$ magnitudes,

* E-mail: a.karapetyan@yerphi.am

and other parameters. For the current study, we selected only normal, 91T-, and 91bg-like SN Ia subclasses, which include a sufficient number of events from a statistical perspective.

For hosts, we restricted to Sab–Scd morphologies since we are interested in studying SNe Ia in galaxies with well-developed arms, where spiral DWs play an important role (e.g. Elmegreen & Elmegreen 1987; Pour-Imani et al. 2016; Karapetyan et al. 2018). Following the approach of Hakobyan et al. (2014), we visually checked the levels of morphological disturbances of the host galaxies using their images from different surveys. The hosts with interacting and merging attributes were excluded from the sample since we are interested in studying SNe Ia in non-disturbed spiral galaxies. In addition, to avoid projection and absorption effects in the discs due to high inclinations, as well as to accurately investigate the immediate vicinity of SNe in terms of the existence of host spiral arms, the sample is limited to galaxies with $i < 60^\circ$. Only 142 SNe Ia in 137 host galaxies met the applied restrictions.

In spiral galaxies, the vast majority of SNe Ia belonging to normal, 91T-, and 91bg-like subclasses are discovered in disc of hosts (Hakobyan et al. 2021). Given this and using SN coordinates on the g -band images,¹ for each SNe Ia we visually inspected the area of a circular ring in a quadrant of host disc, where the SN is discovered, in terms of presence of well-pronounced spiral arms. This is important because we aimed to link SN progenitors to a population of stars born due to the SF after passing and compressing gas clouds through the DW (e.g. Mikhailova et al. 2007; A16). SNe Ia in the circumnuclear region or in the far outer disc (SN galactocentric distance $< 0.1 R_{25}$ or $> R_{25}$) were excluded from this study,² as well as those visually identified within the radius swept up by host galactic bar. As a result of this selection, we were finally left with 77 SNe Ia in 74 host galaxies (see Table A1).

We determined the host spiral arm structures and the SNe positions with respect to the spiral arms according to the approaches detailed in A16. In short, we defined *arm* and *interarm* SNe Ia that are discovered inside the host arm edges or in the interarm region, respectively. To accomplish this, we used the residual images of the host galaxies after subtraction of the fitted $r^{1/4}$ bulge+exponential disc profiles from the smoothed g -band fits images. In the residual images, the values of the interarm pixels are negative, since the fitted profiles use fluxes from both the arm and interarm regions. Similar to A16, we fixed the edges of the spiral arms when the flux values change the sign. Fig. 1 shows examples of original and bulge+disc subtracted images of galaxies that host arm and interarm SNe Ia. Table A2 lists the numbers of SNe Ia in arm and interarm subsamples.

For each SNe Ia in the subtracted images, we measured the distance (d) from the g -band surface brightness peak of the nearest spiral arm through the galactocentric direction (b_s distance in Fig. 2). Only for two cases (SN1997cw and SN2002ck), the interarm SN association with the nearest spiral arm is somewhat ambiguous. Following A16, we normalized d to the corresponding semiwidth of the spiral arm, i.e. $\tilde{d} = d/W_{\pm}$, to compensate for the various linear sizes of the arm width. The semiwidth is the distance from the spiral arm peak to the inner/outer edge of the arm through the galactocentric direction. The W_- is the inner semiwidth (b_a length in Fig. 2) with negative sign when SN is located between the nearest spiral arm peak and the host galaxy nucleus, and the W_+ is the outer semi-

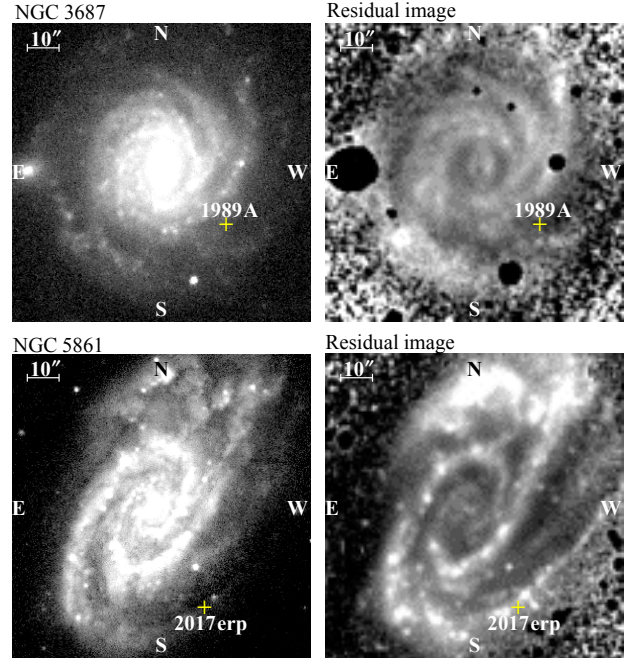


Figure 1. Upper panels: SDSS g -band image of *interarm* SN 1989A host galaxy (left) and its residual image (right), after subtracting bulge and disc components. Bottom panels: Pan-STARRS g -band image of *arm* SN 2017erp host (left) and its residual image (right). The locations of SNe are signed by crosses in all images (north is up and east to the left). Names of host galaxies are noted. In the residual images, bright projected stars are masked.

width (b_c length in Fig. 2) with positive sign when the arm peak is between SN and the nucleus (see A16, for details).

It is worth noting that, according to the DW theory (e.g. Lin & Shu 1964; Roberts 1969), SF activities usually take place at a shock front around the inner edges of spiral arms inside the corotation radius (R_C), and around the outer edges of arms outside the corotation (see Fig. 2). For each SNe Ia, we also measured the distance (D) from the shock front of spiral arm through the galactocentric direction (a_s and c_s distances in Fig. 2 inside and outside R_C radius, respectively). We normalized D to the width (W) of the spiral arm (a_c length in Fig. 2), i.e. $\tilde{D} = D/W$.

In addition, we estimated the deprojected galactocentric distances of SNe Ia (R_{SN}), using well-known approach of correction for the host galactic disc inclination (see Hakobyan et al. 2016, for details). This requires the offsets of SNe from the nucleus of host galaxies ($\Delta\alpha$ and $\Delta\delta$), the position angles and inclinations of the discs. Eventually, for each SNe Ia, the R_{SN} is normalized to the g -band R_{25} , i.e. $\tilde{r}_{SN} = R_{SN}/R_{25}$, to compensate for the various linear sizes of hosts. Note that the mentioned parameters are not listed in H20, however they were compiled and/or estimated at the time of that study and are now available in the online database of this Letter.

Table A3 contains new database of this paper on all 77 individual SNe Ia (SN name, *arm* and *interarm* SN definition, \tilde{d} , \tilde{D} , \tilde{r}_{SN}), while H20 contains data on the spectroscopic subclasses and B -band Δm_{15} of the events, as well as data on host galaxies.

¹ We used the FITS images from the Sloan Digital Sky Survey (SDSS; sdss.org), the SkyMapper (skymapper.anu.edu.au), and the Pan-STARRS (outerspace.stsci.edu/display/PANSTARRS) surveys.

² R_{25} is the g -band 25th magnitude isophotal semi-major axis of the disc.

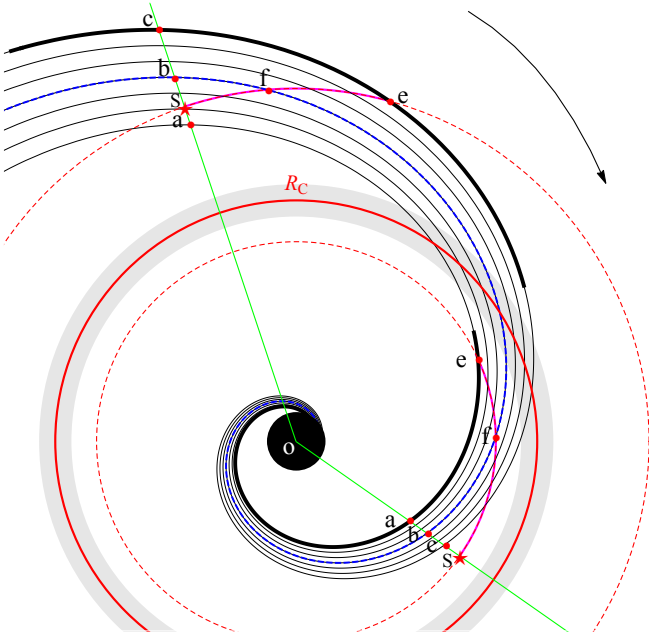


Figure 2. A scheme of grand-design galaxy with logarithmic arms (only one arm is shown), where additional SF is triggered by DWs. The arrow indicates the galaxy’s rotational direction around nucleus (o). Thick black and blue dashed curves present shock fronts of spiral arm and arm’s density (brightness) peak, respectively. A broad gray ring and a red solid circle indicate the corotation region and radius R_C , respectively. Two orbits of SN progenitors are represented by red dashed circles. The purple arc depicts traveled distance of an SN progenitor from birthplace (e) up to the explosion (s), through the arm peak (f) in the particular cases. The radial directions connecting SNe and nucleus are shown by green lines. The a_c , b_a , and b_c lengths are full, inner, and outer (semi)widths of the arm, respectively.

3 RESULTS AND DISCUSSION

3.1 SNe Ia in arm and interarm regions of spiral galaxies

Fig. 3 presents the cumulative Δm_{15} distributions of all sampled SNe Ia in arm and interarm regions. The inset in Fig. 3 shows the same distributions, but only for normal SNe Ia. To statistically compare the distributions, we use nonparametric methods (e.g. Engmann & Cousineau 2011): the two-sample Kolmogorov–Smirnov (KS) and Anderson–Darling (AD) tests.³ The P -values of the tests in Table 1 indicate that the two Δm_{15} distributions, being compared for all sampled SNe Ia, are significantly different. For each SN Ia subclass, we also try to perform the same comparison. However, this can only be done for normal SNe Ia, while the numbers are insufficient for 91T- and 91bg-like events (see Table A2). As for all SNe Ia, the tests’ results show that the Δm_{15} distributions of normal SNe Ia in arm and interarm regions are inconsistent significantly (with only barely AD test significance): the Δm_{15} values of arm SNe Ia are, on average, smaller (slower declining LCs) in comparison with those of interarm SNe Ia (faster declining LCs).

The results presented above can be interpreted within the framework of DW theory (e.g. Lin & Shu 1964; Roberts 1969) and WD explosion models with a sub- M_{Ch} (Shen et al. 2017, 2021). Accord-

³ Due to the small number statistics, to get a better estimate of the P -value of the KS and AD tests, we employ Monte Carlo (MC) simulation with 10^5 iteration, as explained in detail in H20. The threshold for the tests has traditionally been set at a 5 per cent significance level.

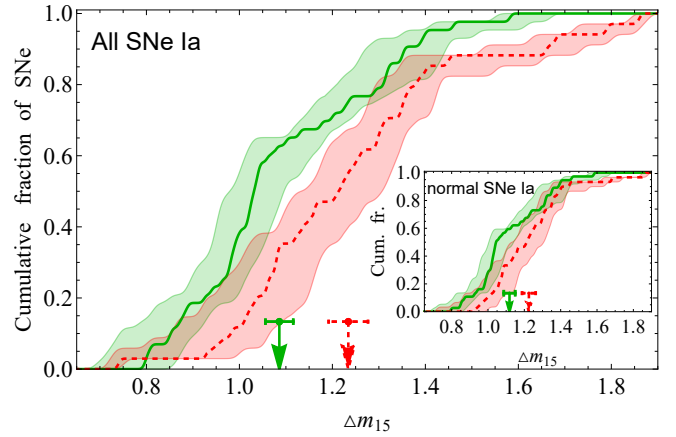


Figure 3. Cumulative Δm_{15} distributions of all arm (green solid) and interarm SNe Ia (red dashed). The associated spreads for each cumulative curve are shown by colored regions, taking into account the uncertainty in Δm_{15} values. Arrows show the mean values (with their standard errors) of the distributions. The inset is the same but only for normal SNe Ia.

Table 1. Comparison of the LC decline rate distributions of arm and interarm SNe Ia.

| SN | $N_{\text{arm SN}}$ | $\langle \Delta m_{15} \rangle$ versus | $N_{\text{interarm SN}}$ | $\langle \Delta m_{15} \rangle$ | $P_{\text{KS}}^{\text{MC}}$ | $P_{\text{AD}}^{\text{MC}}$ |
|--------|---------------------|--|--------------------------|---------------------------------|-----------------------------|-----------------------------|
| All | 43 | 1.09 ± 0.03 versus | 34 | 1.23 ± 0.04 | 0.006 | 0.005 |
| Normal | 37 | 1.12 ± 0.03 versus | 30 | 1.21 ± 0.04 | 0.037 | 0.075 |

Notes. The Δm_{15} mean values and their standard errors for each sample are presented. MC simulation with 10^5 iteration is used to provide $P_{\text{KS}}^{\text{MC}}$ and $P_{\text{AD}}^{\text{MC}}$ probabilities for the KS and AD tests. Differences in the distributions that are statistically significant ($P \leq 0.05$) are marked in bold.

ing to the DW theory, stars (or SN Ia progenitors) were born around shock fronts of spiral arms (birthplace e in Fig. 2) and migrate in the same direction as the disc rotation relative to the spiral pattern (traveled distance eS). In comparison with arm SNe Ia, interarm SNe Ia should have, on average, longer lifetime of their progenitors to travel from the birthplace through the entire arm and explode in interarm regions. Therefore, it can be assumed that interarm SNe Ia originates from an older progenitors than those in arms. The arm/interarm separation thus provides an effective way to distinguish, on average, between younger and older SN Ia progenitors.

On the other hand, as mentioned in the Introduction, in sub- M_{Ch} explosion models (e.g. Sim et al. 2010; Blondin et al. 2017) the Δm_{15} of SN Ia is correlated with the age of the progenitor system (larger Δm_{15} values - older progenitors; Shen et al. 2017, 2021). The described link, together with what is indicated in the paragraph above, allows us to assume that interarm SNe Ia come, on average, from older stellar population with faster declining LCs in contrast to arm SNe Ia.

3.2 The distribution of SNe Ia relative to spiral arms

To supplement and develop the results obtained in the previous section, it is preferable to analyse continuous parameter distributions, such as the galactocentric radii of SNe and their distances from the host spiral arm, and relate them with SN LC decline rates rather than utilizing the arm and interarm discrete binning of SNe Ia.

In this context, a negative radial gradient of stellar population age seen in spiral discs (e.g. González Delgado et al. 2015) prompts us

Table 2. Results of Spearman’s rank correlation tests for different continuous parameters of SNe Ia.

| SN | N_{SN} | Par. 1 versus Par. 2 | r_s | P_s^{MC} |
|--------|-----------------|--|--------|-------------------|
| All | 77 | Δm_{15} versus \tilde{r}_{SN} | 0.032 | 0.783 |
| Normal | 67 | Δm_{15} versus \tilde{r}_{SN} | -0.021 | 0.867 |
| All | 77 | \tilde{d} versus \tilde{r}_{SN} | 0.330 | 0.003 |
| Normal | 67 | \tilde{d} versus \tilde{r}_{SN} | 0.370 | 0.002 |
| All | 77 | Δm_{15} versus \tilde{D} | 0.288 | 0.011 |
| Normal | 67 | Δm_{15} versus \tilde{D} | 0.280 | 0.022 |
| All | 77 | Δm_{15} versus $ \tilde{d} $ | 0.183 | 0.111 |
| Normal | 67 | Δm_{15} versus $ \tilde{d} $ | 0.077 | 0.360 |

Notes. Spearman’s coefficient ($-1 \leq r_s \leq 1$) is a measure of rank correlation. The test’s null hypothesis is that the variables are independent, whereas the alternate hypothesis is that they are not. The permutations with 10^5 MC iterations are used to generate the P_s^{MC} values. Statistically significant correlations are marked in bold ($P \leq 0.05$).

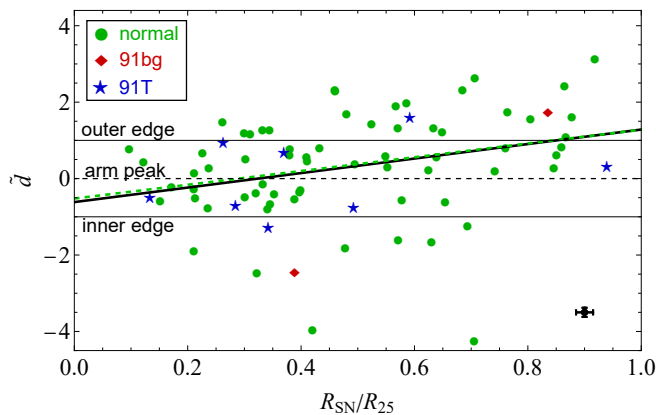


Figure 4. Distribution of the distances of SNe Ia relative to the peaks of spiral arms versus the deprojected and normalized galactocentric distance. The inner and outer edges (solid lines), as well the peak of spiral arm (dashed line) are shown by parallel lines. The best fits for all and normal SN subclass are presented by the solid- and dashed-thick lines, respectively. The error bars in the bottom-right corner display the typical measurement errors.

to check the dependency between the Δm_{15} and \tilde{r}_{SN} of SNe Ia. This dependency has been studied extensively in the past, but no significant correlation has been found (e.g. Gallagher et al. 2005; Galbany et al. 2012; Uddin et al. 2017; Hakobyan et al. 2021). For different subsamples of our study, the Spearman’s rank test in Table 2 also shows not significant trends between the mentioned parameters. In our recent study (Hakobyan et al. 2021), we explained this negative result by the observed fact that in stacked spiral discs the azimuthally averaged stellar population age radially varies only from around 10 down to 8.5 Gyr from the center to the periphery (e.g. González Delgado et al. 2015). While a significant correlation is observed between the LC decline rate and the global ages of hosts (the ages range approximately from 1 to 10 Gyr, Gupta et al. 2011; Pan et al. 2014; Campbell et al. 2016; H20). The relatively narrower radial age range is most likely the reason why the Δm_{15} versus \tilde{r}_{SN} correlation cannot be well-observed.

However, we can uncover an important relationship between host stellar population and properties of SNe Ia progenitors by looking at the distribution of SNe Ia relative to spiral arms of galaxies (e.g. Petrosian et al. 2005; Mikhailova et al. 2007; A16). The relation between the normalized distances \tilde{d} of SNe Ia from the arm peak

and their deprojected and normalized galactocentric distances \tilde{r}_{SN} are shown in Fig 4. There is a positive trend between the parameters, as shown by the fit line to the data. The Spearman’s rank correlation test in Table 2 indicates that this trend is statistically significant for all and normal SNe Ia samples. In A16, the corresponding trend was not significant, probably because of approximately 3.5 times smaller sample of SNe Ia and their different selection criteria for hosts and SN Ia subclasses.

In Fig 4, the fit line to the distances of SNe Ia relative to the arm peak intersects with the arm roughly at a value of 0.35 in units of isophotal radii. Since direct measurements of the corotation radii of host galaxies are not available for the current sample, we examine the averaged value of R_C for seven host galaxies of SNe Ia from our previous paper Karapetyan et al. (2018). These galaxies’ averaged morphological type, Sbc, agrees well with that of the host galaxy sample used in the current study (Table A1). Moreover, the mean $R_C \approx 0.38 \pm 0.05$ for the mentioned sample from Karapetyan et al. is in good agreement with the intersection point in Fig 4. Therefore, this intersection point 0.35 can be adopted as an average corotation radius for our hosts in units of isophotal radii.

The findings in Fig 4 can be interpreted in the context of the DW theory where the steady waves in grand-design galaxies have a strong influence on triggering SF processes close to the shock fronts of spiral arms (e.g. Lin & Shu 1964; Roberts 1969, see also Fig. 2). This is supported by the mentioned quantitative agreement for the average corotation radius of hosts and the observational fact that the SNe Ia explosion sites are mainly distributed around the inner and outer edges of the arms (shock fronts) inside and outside the corotation radius, respectively. Such locations of SNe Ia may be due to a combination of the circular velocity of progenitors in the disc relative to the pattern speed of the spiral arms (e.g. A16) and the ages of SN Ia progenitors (e.g. Childress et al. 2014). Long lived progenitors could travel farther by their circular orbits from the birthplaces around the shock fronts to the explosion sites. Inside the corotation radius this circular direction is from the inner to outer edges, while outside the corotation the direction is from the outer to inner edges of arms (e.g. e_s arcs in Fig 2). Given that spiral galaxies are outnumbered by short-lived (prompt, i.e. 200-500 Myr) SN Ia progenitors (e.g. Raskin et al. 2009; Childress et al. 2014), we observe their distribution close to their birthplaces around the shock fronts.

From the above described DW scenario, we can assume that the traveled circular distance of SN progenitor is an indicator of their age. On the other hand, from the e_{sc} (e_{sa}) curvilinear triangle outside (inside) the corotation in Fig 2, it can be understood that the s_c (s_a) distance is proportional to the e_s distance. Here, the s_c (or s_a) is the distance of SN Ia from the shock front of spiral arm through the galactocentric direction, which we measured in Section 2 and normalized to the arm width (i.e. \tilde{D}), while the e_s is the traveled circular distance of SN progenitor.

Considering that SNe Ia LC decline rate can also be an age indicator for the progenitors in sub- M_{Ch} explosion models, in Table 2 and Fig 5 we study the correlations between Δm_{15} values and \tilde{D} distances from the shock fronts of host spiral arms. The corresponding P_s values in Table 2 show that there are significant correlations between these parameters. The result enables us to draw the conclusion that, on average, the progenitors of SNe Ia with smaller Δm_{15} values have shorter lifetimes and thus traveled shorter distances from the shock fronts, i.e. birthplace, in contrast to progenitors with larger Δm_{15} values, which have longer lifetimes and thus traveled farther away from the shock fronts.

The correlation tests in Table 2 show the positive trend between the Δm_{15} of SNe Ia and their measured distances from the arm peak,

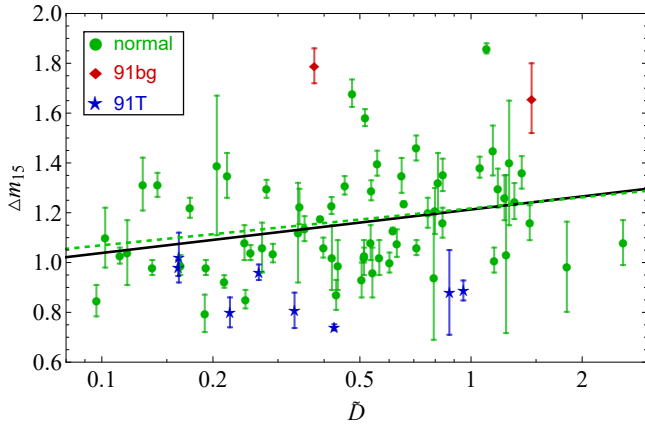


Figure 5. Distributions of Δm_{15} values of SNe Ia versus \tilde{D} distances from the shock fronts of host spiral arms. The best fits for all and normal SN subclass are presented by the solid- and dashed-thick lines, respectively.

which might be assumed from the result of the Δm_{15} differences between SN Ia in arm/interarm regions. However, the P_s values of the test show that this trend is not statistically significant. This insignificance likely caused by the blurs in $|\tilde{d}|$ as a lifetime indicator in the distribution of Δm_{15} versus $|\tilde{d}|$, because the SN distance from the arm peak does not represent the progenitors' traveled distance during entire lifetime (till to SN explosion): the spiral arm peak cannot be considered as a main birthplace of progenitors of SNe Ia.

It is worth noting that when conducting all statistical tests of our study without two SNe Ia with ambiguous association with the nearest spiral arm (see Section 2), all the results of the *Letter* and their significance remain unchanged.

4 CONCLUSIONS

In this *Letter*, using a sample of Sab–Scd galaxies hosting 77 SNe Ia and our measurements of the SN distances from the nearby spiral arms, we perform an analysis of the SNe distribution relative to host arms and study their LC decline rates (Δm_{15}). We demonstrate that the Δm_{15} values of *arm* SNe Ia are typically smaller (slower declining) than those of *interarm* SNe Ia (faster declining). We show that the SN distances from the spiral arms and their galactocentric radii are correlated: before and after the average corotation radius, SNe Ia are located near the inner and outer edges (shock fronts) of spiral arms. For the first time, we find a correlation between Δm_{15} values and the SN distances from the shock fronts of the arms. The results can be interpreted within the frameworks of DW theory, where SN progenitors were born around shock fronts of spiral arms and migrate crossing the spiral pattern to the explosion sites, and WD explosion models with sub- M_{Ch} , where SN LC decline rate is an indicator of progenitor age. On average, the progenitors of SNe Ia with smaller Δm_{15} values have shorter lifetimes and thus traveled shorter distances from the shock fronts, i.e. birthplace, in contrast to progenitors with larger Δm_{15} values, which have longer lifetimes and thus traveled farther away from the shock fronts.

As our study used a small sample size, we encourage new statistically more powerful studies with larger and more robust datasets of SNe Ia and their hosts (e.g. integral field observations, with available corotation radii) to better constrain the nature of SN Ia progenitor.

ACKNOWLEDGEMENTS

We appreciate the anonymous referee for comments towards improving our *Letter*. I am grateful for the help of my PhD supervisor, Dr. Artur Hakobyan. The work was supported by the Science Committee of RA, in the frames of the research project № 21T–1C236.

DATA AVAILABILITY

The online version of this *Letter* contains the data underlying this study (see Table A3, for instructions).

REFERENCES

- Aramyan L. S., et al., 2016, *MNRAS*, **459**, 3130 (A16)
 Blondin S., Dessart L., Hillier D. J., Khokhlov A. M., 2017, *MNRAS*, **470**, 157
 Campbell H., Fraser M., Gilmore G., 2016, *MNRAS*, **457**, 3470
 Childress M. J., Wolf C., Zahid H. J., 2014, *MNRAS*, **445**, 1898
 Elmegreen D. M., Elmegreen B. G., 1987, *ApJ*, **314**, 3
 Engmann S., Cousineau D., 2011, *J. Appl. Quant. Methods*, **6**, 1
 Galbany L., et al., 2012, *ApJ*, **755**, 125
 Gallagher J. S., Garnavich P. M., Berlind P., Challis P., Jha S., Kirshner R. P., 2005, *ApJ*, **634**, 210
 González Delgado R. M., et al., 2015, *A&A*, **581**, A103
 Gupta R. R., et al., 2011, *ApJ*, **740**, 92
 Hakobyan A. A., et al., 2014, *MNRAS*, **444**, 2428
 Hakobyan A. A., et al., 2016, *MNRAS*, **456**, 2848
 Hakobyan A. A., Barkhudaryan L. V., Karapetyan A. G., Gevorgyan M. H., Mamon G. A., Kunth D., Adibekyan V., Turatto M., 2020, *MNRAS*, **499**, 1424 (H20)
 Hakobyan A. A., Karapetyan A. G., Barkhudaryan L. V., Gevorgyan M. H., Adibekyan V., 2021, *MNRAS*, **505**, L52
 Karapetyan A. G., Hakobyan A. A., Barkhudaryan L. V., Mamon G. A., Kunth D., Adibekyan V., Turatto M., 2018, *MNRAS*, **481**, 566
 Lin C. C., Shu F. H., 1964, *ApJ*, **140**, 646
 Livio M., Mazzali P., 2018, *Phys. Rep.*, **736**, 1
 Mikhailova G. A., Bartunov O. S., Tsvetkov D. Y., 2007, *Astron. Lett.*, **33**, 715
 Pan Y. C., et al., 2014, *MNRAS*, **438**, 1391
 Petrosian A., et al., 2005, *AJ*, **129**, 1369
 Phillips M. M., 1993, *ApJ*, **413**, L105
 Phillips M. M., Lira P., Suntzeff N. B., Schommer R. A., Hamuy M., Maza J., 1999, *AJ*, **118**, 1766
 Pour-Imani H., Kennefick D., Kennefick J., Davis B. L., Shields D. W., Shameer Abdeen M., 2016, *ApJ*, **827**, L2
 Raskin C., Scannapieco E., Rhoads J., Della Valle M., 2009, *ApJ*, **707**, 74
 Rigault M., et al., 2020, *A&A*, **644**, A176
 Roberts W. W., 1969, *ApJ*, **158**, 123
 Shen K. J., Toonen S., Graur O., 2017, *ApJ*, **851**, L50
 Shen K. J., Blondin S., Kasen D., Dessart L., Townsley D. M., Boos S., Hillier D. J., 2021, *ApJ*, **909**, L18
 Sim S. A., Röpké F. K., Hillebrandt W., Kromer M., Pakmor R., Fink M., Ruiter A. J., Seitenzahl I. R., 2010, *ApJ*, **714**, L52
 Taubenberger S., 2017, in Alsabti A. W., Murdin P., eds, *The Extremes of Thermonuclear Supernovae, Handbook of Supernovae*. Springer, Cham, p. 317
 Uddin S. A., Mould J., Lidman C., Ruhlmann-Kleider V., Zhang B. R., 2017, *ApJ*, **848**, 56

APPENDIX A: ONLINE MATERIAL

Table A1 shows morphological distribution of the sampled SNe Ia host galaxies, split between different SN subclasses. The numbers

Table A1. Morphological distribution of the sampled SNe Ia host galaxies, split between different SN subclasses.

| SN | Sab | Sb | Sbc | Sc | Scd | All |
|--------|-----|----|-----|----|-----|-----|
| Normal | 6 | 18 | 25 | 17 | 1 | 67 |
| 91T | 2 | 0 | 4 | 2 | 0 | 8 |
| 91bg | 2 | 0 | 0 | 0 | 0 | 2 |
| ALL | 10 | 18 | 29 | 19 | 1 | 77 |

Table A2. Numbers of *arm* and *interarm* SNe Ia within Sab–Scd galaxies, split between different SN subclasses.

| SN | <i>arm</i> | <i>interarm</i> |
|--------|------------|-----------------|
| Normal | 37 | 30 |
| 91T | 6 | 2 |
| 91bg | 0 | 2 |
| All | 43 | 34 |

Table A3. The database of 77 SNe Ia of the study. The first ten entries are presented, while the entire table are available online.

| SN | Arm/interarm definition | \tilde{d} | \tilde{D} | \tilde{r}_{SN} |
|--------|-------------------------|-------------|-------------|-------------------------|
| 1989A | interarm | 1.442 | 0.272 | 0.524 |
| 1989B | arm | 0.220 | 0.420 | 0.171 |
| 1990N | arm | 0.830 | 0.117 | 0.859 |
| 1990O | interarm | 1.753 | 0.541 | 0.764 |
| 1995al | arm | 0.516 | 0.601 | 0.302 |
| 1995E | arm | 0.478 | 0.398 | 0.411 |
| 1996ai | arm | 0.584 | 0.163 | 0.151 |
| 1996bo | arm | 0.445 | 0.537 | 0.122 |
| 1996Z | interarm | 1.226 | 0.173 | 0.649 |
| 1997bp | interarm | 2.326 | 0.837 | 0.459 |

of *arm* and *interarm* SNe Ia within Sab–Scd galaxies are shown in Table A2.

Table A3 shows the first ten rows of the data used in our *Letter*. A CSV file containing the whole table is available online.